Journal of Translational Autoimmunity 3 (2020) 100060

Contents lists available at ScienceDirect

Journal of Translational Autoimmunity

journal homepage: www.journals.elsevier.com/journal-of-translational-autoimmunity/

Inflammatory monocyte-derived dendritic cells mediate autoimmunity in murine model of systemic lupus erythematosus

Fumi Miyagawa [a,*], Yutaka Tagaya [b], Keiko Ozato [c], Kyoji Horie [d], Hideo Asada [a]

[a] Department of Dermatology, Nara Medical University School of Medicine, 840 Shijo, Kashihara, Nara, 634-8522, Japan
[b] Cell Biology Lab, Division of Infectious Agents and Cancer, Institute of Human Virology, University of Maryland School of Medicine, Baltimore, MD, 21201, USA
[c] Laboratory of Molecular Growth Regulation, National Institute of Child Health and Human Development, National Institutes of Health, Bethesda, MD, 20892, USA
[d] Department of Physiology II, Nara Medical University School of Medicine, 840 Shijo, Kashihara, Nara, 634-8522, Japan

ARTICLE INFO

Keywords:
SLE
Inflammatory monocyte
Monocyte-derived DC
IRF7
IRF8

ABSTRACT

Using a mouse model of systemic lupus erythematosus (SLE), we recently demonstrated that the two major manifestations of SLE are mechanistically independent because the type I IFN pathway leads to the autoantibody production whereas the NF-κB activation is sufficient for the development of glomerulonephritis. To further advance our understandings on the molecular pathways regulating the development of SLE, we studied the role of IRF8 because it controls both type I IFN and NF-κB pathways and saw that IRF8-deficient mice failed to develop either glomerulonephritis or the autoantibody production. Furthermore, these genetically engineered mice prompted us to realize the important role of Ly6C^{high} inflammatory monocytes in the development of SLE. These monocytes migrate to the peritoneal cavity in WT and IRF7-deficient mice but not in IRF8-deficient mice, and there they produce both type I IFN and proinflammatory cytokines in WT mice, while in IRF7-deficient mice they only produce proinflammatory cytokines. Upon migration to the spleen, Ly6C^{high} inflammatory monocytes differentiate into dendritic cells (DCs) which are capable of producing proinflammatory cytokines in response to dsDNA autoantigen. Collectively, type I IFN produced from inflammatory monocytes/monocyte-derived DCs might be essential for autoantibody production whereas proinflammatory cytokines produced from them might mediate tissue damages in this model. Our study reveals a specialized role for monocyte-derived antigen presenting cells in autoimmunity. Plasticity of monocyte might play an important role not only in the pathogenesis of the disease but also in flare-ups of the disease.

1. Introduction

Systemic lupus erythematosus (SLE) is a multisystem autoimmune disease characterized by the loss of immune tolerance to nuclear autoantigens resulting in the production of pathogenic autoantibodies that cause inflammation and tissue damage to multiple organs. In the development of SLE, three main immune pathways have been identified: aberrant clearance of nucleic-acid-containing debris and immune complexes, excess innate immune activation involving Toll-like receptors (TLRs) and type I interferons (IFNs) and dysfunctional response of T and B lymphocytes [1,2]. Genetic association studies revealed that aberrant regulation of innate and adaptive immunity genes contribute to the pathogenesis of SLE [3]. Included are IRF7 and IRF8 [3], both of which belong to the IFN regulatory factor family [4] and were characterized as transcriptional regulators of type I IFN (IFN-α, IFN-β) and IFN-stimulated genes (ISGs). In addition, they play a pivotal role in various aspects of immune responses [4]. IRF7 is considered to be a master regulator of type I IFN-dependent immune responses [5]. In contrast, IRF8 controls the lineage commitment between the myeloid and B cells [4], DC development and function [6], a silencing program for Th17 cell differentiation [7], and the differentiation of naïve CD8 T cells into effector cells [8]. However, the precise role of IRF7 and IRF8 in the SLE pathogenesis is still under investigation.

Using a murine model of SLE induced by 2,6,10,14-tetramethylpentadecane (TMPD, pristane), we previously reported that IRF7-deficient mice developed glomerulonephritis while they failed to produce autoantibodies against ssDNA, dsDNA, Sm, and RNP [9]. We demonstrated two major disease manifestations of SLE can be molecularly uncoupled, in that IRF7/type I IFN pathway is essential for autoantibody production while the NF-κB pathway sufficiently controls the development of

* Corresponding author.
E-mail address: fumim@naramed-u.ac.jp (F. Miyagawa).

https://doi.org/10.1016/j.jtauto.2020.100060
Received 1 June 2020; Received in revised form 18 June 2020; Accepted 8 July 2020

glomerulonephritis [9].

In order to understand the role of IRF8 in SLE, we challenged IRF8-deficient mice with TMPD. Curiously, IRF8-deficient mice displayed no production of autoantibodies along with reduced glomerulonephritis after the TMPD injection. Inflammatory monocytes are important component of this SLE model because they produce proinflammatory cytokines and thereby facilitating the production of autoantibodies and glomerulonephritis [10,11].

However, inflammatory monocytes were not induced by TMPD in IRF8-deficient mice. Furthermore, similar cells induced by TMPD in IRF7-deficient mice failed to produce type I IFN, critically suggesting the unique contribution of IRF7 and IRF8 in the generation of competent proinflammatory monocytes and their IFN production. When differentiated into $CD11c^{+}$ DCs *in vivo*, these cells are capable of producing proinflammatory cytokines in response to dsDNA which play a major role in tissue damages that ensue. Thus, proinflammatory monocytes appear to be the missing link in our experimental model between IRF7/8 and SLE by way of the production of type I IFNs.

One typical characteristic of SLE is the fluctuation in time of disease activity [12]. We hypothesize that this fluctuation may synchronize with the intermittent production of inflammatory monocytes/monocyte-derived DCs *in vivo*. Our study also suggests targeting monocyte migration/homing by using chemoattractants or their inhibitors as a potential therapeutic intervention in patients with SLE.

2. Materials and methods

2.1. Mice

C57BL/6 mice (wild-type; WT), *Irf7*$^{-/-}$ mice, and CD45.1 mice were purchased from CLEA Japan (Tokyo), RIKEN BRC (Tsukuba), and the Jackson Laboratory (Bar Harbor, ME), respectively. *Irf8*$^{-/-}$ mice [13] were obtained from Dr. Keiko Ozato (National Institute of Child Health and Human Development, National Institutes of Health, Bethesda, MD, USA). CD45.1^{+}*Irf7*$^{-/-}$ mice were generated by backcrossing CD45.1 mice with *Irf7*$^{-/-}$ mice. The mice were housed in a specific pathogen-free facility and bred and used in accordance with protocols approved by the Animal Care and Use Committee of the Nara Medical University.

2.2. Intraperitoneal injection of TMPD

Male and female mice between 8 and 16 weeks old were used. Age and gender matched WT, *Irf7*$^{-/-}$, or *Irf8*$^{-/-}$ mice were given a single i.p. injection of 0.5 ml of TMPD (pristane) (Funakoshi, Tokyo) or PBS (vehicle). Ten months later, urine, blood, and kidneys were harvested. In some experiments, blood, kidneys and peritoneal cells were harvested two weeks after injection.

2.3. Measurement of urine protein

Proteinuria was assessed by a urinary test strip (Wako, Osaka) and graded as 0 (none), 1+ (trace; 10–20 mg/dl), 2+ (30 mg/dl), 3+ (100 mg/dl), 4+ (300 mg/dl), and 5+ (>1000 mg/dl).

2.4. Direct immunofluorescence

Kidneys from WT, *Irf7*$^{-/-}$, or *Irf8*$^{-/-}$ mice treated with TMPD or PBS were harvested 10 months after the disease induction, frozen in OCT medium, and stored at −80 °C. Cryosections were prepared at 6 μm thickness and incubated with FITC-anti-mouse IgG Ab (SouthernBiotech, Birmingham, AL), or Alexa Fluor 488-anti-mouse C3 Ab (Novus Biologicals, Littleton, CO). Nuclei were stained with Hoechst 33,258 (ThermoFisher Scientific, Waltham, MA) and examined by fluorescence microscopy (Keyence, Osaka). For the evaluation of glomerular lesions, images of 5 glomeruli per mouse were captured with a constant exposure time on fluorescence microscopy. From captured images, each glomerular lesion was scored based on the involved area as 0 (no staining), 1 (<25%), 2 (25–50%), 3 (50–75%), and 4 (>75%). The average severity grade was calculated and defined as the renal score of the mouse.

For CD11c and CD45.1 double immunofluorescence staining, 6 μm frozen tissue sections of the spleen were fixed with cold acetone, incubated with FITC-CD45.1 (clone A20) (eBiosciences, Tokyo) and PE-CD11c Ab (HL3) (BD pharmingen, Tokyo). In some experiments, double immunofluorescence staining was performed with FITC-CD45.2 Ab (clone 104) (Biolegend, San Diego, CA) and PE-CD11c Ab. The sections were observed by fluorescence microscopy (Keyence).

2.5. Indirect immunofluorescence

Hep2 cells were cultured in 8-well CultureSlide (BD Falcon, Tokyo), fixed with cold acetone, and blocked with 3% BSA and 1% FCS in PBS for 1 h. Sera from the mice 10 months after TMPD or PBS injection were diluted at 1:100 and slides were incubated with diluted sera overnight. Slides were then incubated with FITC-conjugated anti-IgG Ab for 30 min, mounted and examined by fluorescence microscopy (Olympus, Tokyo).

2.6. ELISA

The sera were obtained 10 months after TMPD or PBS injection. Serum concentrations of anti-nuclear antibody (ANA), anti-nRNP Ab (Alpha diagnostic international, San Antonio, TX), and anti-dsDNA Ab (FUJIFILM Wako Shibayagi, Gunma, Japan) were assayed by ELISA. In some experiments, the sera were obtained 2 weeks after injection and the serum levels of TNF-α and IL-6 were determined by ELISA (R&D systems, Minneapolis, MN).

2.7. Harvesting of peritoneal cells

The peritoneal cavity was lavaged with 2 ml of complete RPMI plus 10 U/ml heparin. Cells were collected by centrifugation, depleted of RBC by ACK lysing buffer and then resuspended in complete RPMI.

2.8. Culture of peritoneal cells, lymph node cells, and spleen cells

Freshly isolated peritoneal cells from WT, *Irf7*$^{-/-}$, or *Irf8*$^{-/-}$ mice were grown in complete RPMI in the presence or absence of TMPD. Due to its insolubility in aqueous medium, TMPD was added as the inclusion complexes with β-cyclodextrin (β-CyD; Wako) as described previously [9]. In some experiments, single cell suspensions were prepared from inguinal lymph nodes (LNs) and spleen from three strains and cultured with or without TMPD as described above.

2.9. RNA extraction and real-time PCR

Peritoneal cells were harvested two weeks after TMPD or PBS injection. In some experiments, peritoneal cells were enriched for inflammatory monocytes by negative selection using PE-conjugated mAb against CD3, CD11c, CD19, B220, Ly6G, and anti-PE Microbeads (Miltenyi Biotec, Auburn, CA). Total RNA was extracted from peritoneal cells or inflammatory monocytes using RNAeasy Plus Kit (QIAGEN, Tokyo) and cDNA was synthesized using High Capacity RNA-to-cDNA Kit (Applied Biosystems, Foster City, CA). Real-time PCR was performed using Taqman Fast Advanced Master Mix with Taqman Gene Expression Assays (Applied Biosystems). The data were normalized to the expression levels of GAPDH.

2.10. Evaluation of glomerular cellularity

Kidneys were harvested 10 months after PBS or TMPD injection and fixed in 10% neutral-buffered formalin. Paraffin-embedded tissues were sectioned and stained with hematoxylin and eosin using standard techniques. Glomerular cellularity was evaluated with H&E sections of the

kidneys by counting the number of nuclei per glomerular cross-section as previously described [9].

2.11. Single cell preparation from kidney

Kidney was harvested, diced, and incubated with 0.5 mg/ml Liberase (Roche Applied Science, Branford, CT) and 0.05% DNase (Roche Applied Science) in RPMI at 37 °C for 60 min.

2.12. Antibodies and flow cytometry

FITC-anti-CD3 (clone 145-2C11), IA/IE (2G9), PE-CD69 (H1·2F3), CD11c (HL3), PerCP-Cy5.5-Ly6G (1A8), APC-anti-CD4 (RM4-5), CD11b (M1/70) (BD Pharmingen), Alexa Fluor 488-Ly6C (HK1.4), PE-Ly6G (1A8) (eBioscience), PerCP-anti-CD45.1 (A20), and PerCP-anti-CD45.2 antibody (104) (BioLegend) were used for cell-surface staining. Apoptosis was assessed by staining for FITC-annexin V/PI, and FITC-anti-active caspase 3 (C92-605) according to the manufacturer's protocols (BD Pharmingen). Stained cells were analyzed on a FACSCalibur flow cytometer (Becton Dickinson, Tokyo).

2.13. Sorting

CD45.1 mice (donor) were i.p. injected with TMPD. Two weeks later, peritoneal cells from about 10 CD45.1 mice were harvested, pooled, and enriched for inflammatory monocytes by depleting CD3, CD11c, CD19, B220 cells using PE-conjugated each Ab followed by anti-PE Microbeads. $Ly6C^{high}Ly6G^{-}CD11b^{+}$ inflammatory monocytes were then sorted by gating on cells positive for Ly6C and CD11b and negative for Ly6G with a BD FACSAria II cell sorter (BD Biosciences). To track the fate of $Ly6C^{high}$ monocytes that had migrated into the peritoneal cavity, 1–2x10^5 sorted $CD45.1^{+}$ $Ly6C^{high}Ly6G^{-}CD11b^{+}$ were then i.p. injected into the WT mouse (host) which received TMPD injection intraperitoneally 2 weeks earlier. Similar experiments were performed using $CD45.1^{+}$ *Irf7*$^{-/-}$ mice as donor and *Irf7*$^{-/-}$ mice as host. For cross-over approaches, CD45.1 mice and *Irf7*$^{-/-}$ mice were used as donors, and *Irf7*$^{-/-}$ mice and CD45.1 mice were used as hosts, respectively. The purity of the sorted cells was >95%.

2.14. Intracellular cytokine staining

WT mouse (host) was i.p. injected with TMPD and subsequently received 1–2x10^5 sorted $Ly6C^{high}Ly6G^{-}CD11b^{+}$ cells from CD45.1 mice (donor) 2 weeks later. Six days later, spleen was harvested and cultured at 1 × 10^7 cells/mL in a 24-well bottom plate at 37 °C with 5 μg/ml of Golgiplug (BD Pharmingen) in the presence or absence of calf thymus double-stranded (ds) DNA (Sigma) at 100 μg/ml. Six hours later, cells were harvested and stained for CD45.1 and CD11c. Cells were fixed and permeabilized by incubation with cytofix/cytoperm solution (BD Pharmingen). Cells were then incubated with PE-anti-IL-6 (clone MP6-20F3), PE-TNF-α (MP6-XT22) (BD Pharmingen), PE-IL-1α (ALF-167), and PE-IL-1β (NJTEN3) (eBioscience) and analyzed on a FACSCalibur flow cytometer. Similar experiments were performed with various combination of hosts and donors.

In some experiments, WT and Irf7$^{-/-}$ mice were i.p. injected with TMPD. Two weeks later, peritoneal cells were harvested, cultured as above and stained with Alexa Fluor 488-Ly6C, PerCP-Cy5.5-Ly6G, and APC-CD11b. Cells were then fixed, permeabilized, and stained with anti-IL-6, TNF-α, PE-IL-1α, and PE-IL-1β Abs.

2.15. Statistical analysis

Statistical analyses were carried out using one-way ANOVA with Tukey HSD test and differences of $p < 0.05$ were considered significant.

3. Results

3.1. *Irf7*$^{-/-}$ mice but not *Irf8*$^{-/-}$ mice develop glomerulonephritis

We previously reported that NF-κB pathway-dependent glomerulonephritis still occurred in *Irf7*$^{-/-}$ mice after administration of TMPD [9]. In this study, we determined the contribution of IRF8 to the development of glomerulonephritis because IRF8 controls NF-κB pathway in addition to type I IFN pathway. As previously demonstrated, a single injection of TMPD induces severe proteinuria in wild-type (WT) and *Irf7*$^{-/-}$ mice in 10 months (Fig. 1A) [9]. In contrast, mild to undetectable proteinuria was observed in *Irf8*$^{-/-}$ mice after TMPD injection (Fig. 1A). Histopathology of the kidney revealed glomerular cellularity was increased in WT and *Irf7*$^{-/-}$ mice after TMPD injection but it was normal in TMPD-treated *Irf8*$^{-/-}$ mice (Fig. 1B and C) [9]. The increase in nuclei/glomerulus might be due to inflammation or mesangial cell proliferation in WT and *Irf7*$^{-/-}$ mice. Consistent with these findings, no deposition of IgG and C3 was observed in the glomeruli of *Irf8*$^{-/-}$ mice, while an intense deposition of IgG and C3 were observed in control WT mice (Fig. 1D–G) [9]. *Irf7*$^{-/-}$ mice showed the deposition of IgG but not C3 as we have previously observed (Fig. 1D–G) [9]. Taken together, *Irf8*$^{-/-}$ mice appear refractory to the TMPD challenge in the development of glomerulonephritis, in contrast WT and *Irf7*$^{-/-}$ mice.

Intraperitoneal injection of TMPD has been known to cause lipogranuloma formation in the peritoneum, an ectopic lymphoid tissue that is a site of substantial type I IFN production [14,15]. Interestingly all three strains developed lipogranulomas following the peritoneal TMPD challenge (Supplementary Fig. 1A and B) [9], suggesting that the loss of IRF7 and IRF8 does not deprive cells of their capacity to respond to TMPD.

3.2. Both IRF7 and IRF8 are indispensable for antinuclear antibody production

We next evaluated if antinuclear antibodies (ANAs) are produced in *Irf8*$^{-/-}$ mice. Sera from TMPD-treated WT mice produced either homogeneous or speckled nuclear staining against Hep2 cells by indirect immunofluorescence but sera from *Irf7*$^{-/-}$ mice failed to do so as we previously observed (Fig. 2A) [9]. Sera from *Irf8*$^{-/-}$ mice did not show nuclear staining with Hep2 cells (Fig. 2A), suggesting that anti-nuclear antibodies were not produced in *Irf7*$^{-/-}$ and *Irf8*$^{-/-}$ mice. Similarly, ELISA assay demonstrated the complete lack of ANA, α-dsDNA Ab, and α-RNP Ab in the sera from *Irf7*$^{-/-}$ and *Irf8*$^{-/-}$ mice (Fig. 2B), indicating a crucial requirement of IRF7 or IRF8 for the autoantibody production.

It is well established that activation status of T cells critically controls the humoral response. Thus, we assessed if activation status of CD4 T cells could be compromised in *Irf7*$^{-/-}$ or *Irf8*$^{-/-}$ mice following the TMPD challenge. We found that the expression of an early activation marker, CD69, was significantly reduced on CD4 T cells in *Irf7*$^{-/-}$ mice (Fig. 2C and D). Thus, it is possible that the lack of autoantibody production in *Irf7*$^{-/-}$ mice is caused by the reduced T-cell activation in the absence of IRF7. However, the similar lack of autoantibody production was seen in *Irf8*$^{-/-}$ mice despite significantly more activated T cells being present, suggesting that this mechanism is unlikely.

3.3. Apoptosis was normally induced in *Irf7*$^{-/-}$ and *Irf8*$^{-/-}$ mice

The proposed mechanism by which the TMPD challenge causes the development of lupus-like autoimmunity is its enhancement of cellular apoptosis that provides the autoantigen substrates to help break tolerance [16]. We previously observed that the apoptosis induced by TMPD occurs independent of the autoantibody production in *Irf7*$^{-/-}$ mice [9]. To address the potential mechanisms by which autoantibody production was impaired in *Irf8*$^{-/-}$ mice, we also investigated whether TMPD-induced apoptosis occurs in this strain. We exposed peritoneal exudate cells (PECs) obtained from WT, *Irf7*$^{-/-}$, and *Irf8*$^{-/-}$ mice to

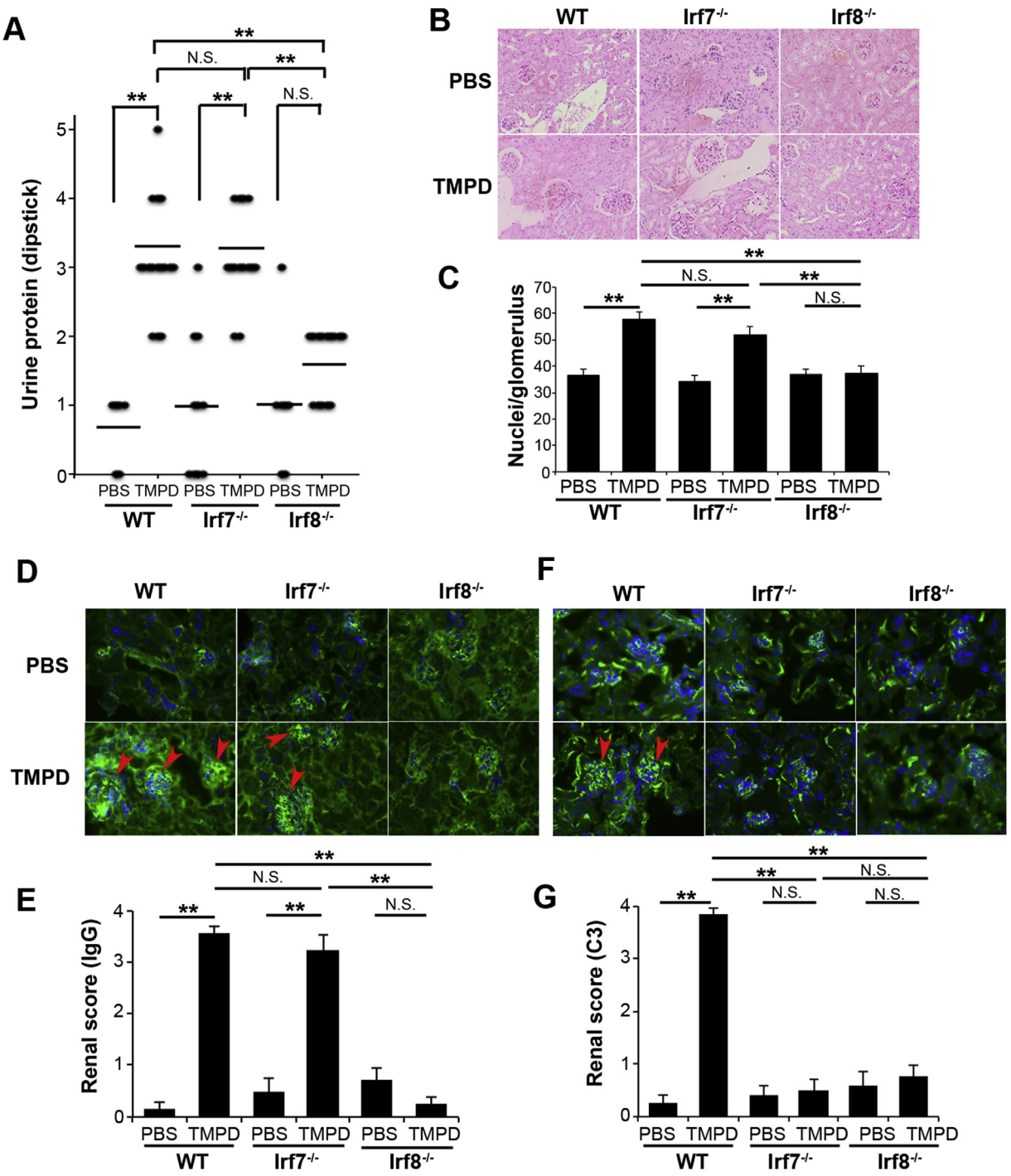

Fig. 1. Lack of the development of glomerulonephritis in *Irf8*$^{-/-}$ mice. (A) Proteinuria occurred in WT and Irf7$^{-/-}$ mice while no major proteinuria was observed with *Irf8*$^{-/-}$ mice 10 Mo after the administration of TMPD. A Horizontal line indicates the mean value in each group (n = 6–10 mice/group for control (PBS), n = 14–18 mice/group for TMPD treatment). **; $p < 0.01$ by one-way ANOVA with Tukey HSD test. N.S. not significant. (B, C) Increased glomerular cellularity in WT and *Irf7*$^{-/-}$ mice but not in Irf8$^{-/-}$ mice following the TMPD injection. Glomerular cellularity was determined as the number of nuclei per glomerular cross-section in tissue sections stained with H&E. Representative images of three independent experiments are shown in (B). The average numbers of nuclei of 20 glomeruli are shown in (C). Error bars represent SEM. **; $p < 0.01$ by one-way ANOVA with Tukey HSD test. N.S. not significant. (D–G) Glomerular IgG (D, E) and C3 (F, G) deposits determined by direct immunofluorescence. Merged immunofluorescence images of anti-IgG Ab or anti-C3 Ab (green) and Hoechst staining (blue). Representative images are shown in (D, F) (x200). Red arrows indicate positive IgG or C3 deposits. Glomerular IgG (E) or C3 (G) deposits were scored from 0 to 4 and the average values from 6 to 11 mice/group were shown (error bars, SEM). **; $p < 0.01$ by one-way ANOVA with Tukey HSD test. N.S. not significant. (D, E) WT and *Irf7*$^{-/-}$ mice treated with TMPD were positive for IgG deposits in glomeruli, while TMPD-treated *Irf8*$^{-/-}$ mice were negative. (F, G) WT mice treated with TMPD were positive for C3 deposits while no C3 staining was observed in *Irf7*$^{-/-}$ and *Irf8*$^{-/-}$ mice. Arrows indicate positive C3 deposits. . (For interpretation of the references to colour in this figure legend, the reader is referred to the Web version of this article.)

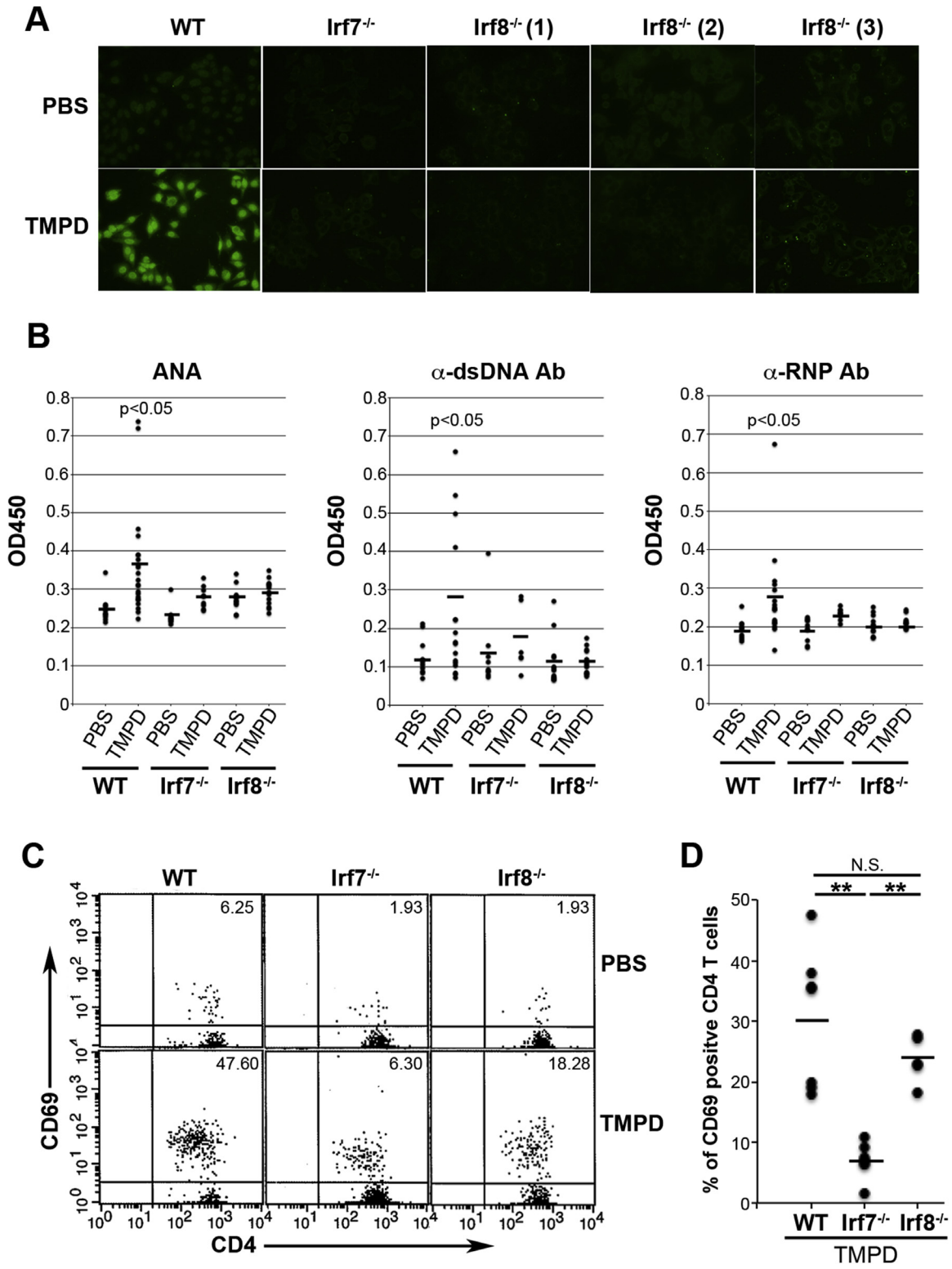

Fig. 2. Lack of the production of autoantibodies in *Irf7*$^{-/-}$ and *Irf8*$^{-/-}$ mice. (A) Detection of antinuclear antibody (ANA) by indirect immunofluorescence using Hep2 cells. Sera were collected at 10 Mo after PBS or TMPD injections and used at 1:100 dilution. ANA was strongly detectable in the sera from TMPD-treated WT mice whereas those from *Irf7*$^{-/-}$ and *Irf8*$^{-/-}$ mice showed no ANA staining. Representative images of five independent experiments are shown. (B) ANA, α-dsDNAAb, and α-RNPAb measured in sera from three strains with PBS or TMPD challenge after 10 Mo by ELISA (sera were used at 1:100 dilution). Antibodies were only present in WT sera 10 Mo after TMPD challenge. A horizontal line indicates the mean values in each group. n = 10–22 mice per group. $p < 0.05$ versus other groups. One-way ANOVA with Tukey HSD test. (C) Representative flow cytometric plots of CD4 and CD69 expression by PECs from three strains 2 weeks after PBS or TMPD injection. Cells were gated on $CD3^+CD4^+$ cells within the lymphocyte population. The percentage of $CD3^+CD4^+CD69^+$ cells is indicated. One representative result of five independent experiments is shown. (D) Quantification of $CD4^+CD69^+$ T cells. Average values from n = 5–7 mice per group are shown. CD4 T cells from *Irf7*$^{-/-}$ mice expressed less CD69 compared to those from WT mice. **; $p < 0.01$ by one-way ANOVA with Tukey HSD test. N.S. not significant.

TMPD/β-CyD. The extracted cells from all strains underwent apoptosis to a similar extent (Fig. 3A and B) [9]. Similarly, TMPD induced apoptosis in other cell types such as LN cells (Fig. 3C) and spleen cells (Fig. 3D), indicating that this effect of TMPD is not specific to PECs. *In vivo* stimulation by TMPD also induced apoptosis in PECs from all strains (Fig. 3E). These results suggest that the autoantigens are equally available in these mice and that dysregulation of apoptosis was not the cause of the lack of the autoantibody production in *Irf7*$^{-/-}$ and *Irf8*$^{-/-}$ mice.

3.4. Recruitment of Ly6C^{high} monocytes in WT and Irf7$^{-/-}$ mice but not in Irf8$^{-/-}$ mice

To explain the previous findings, we postulated that *Irf7*$^{-/-}$ and *Irf8*$^{-/-}$ mice may lack some cellular components that regulate SLE symptoms

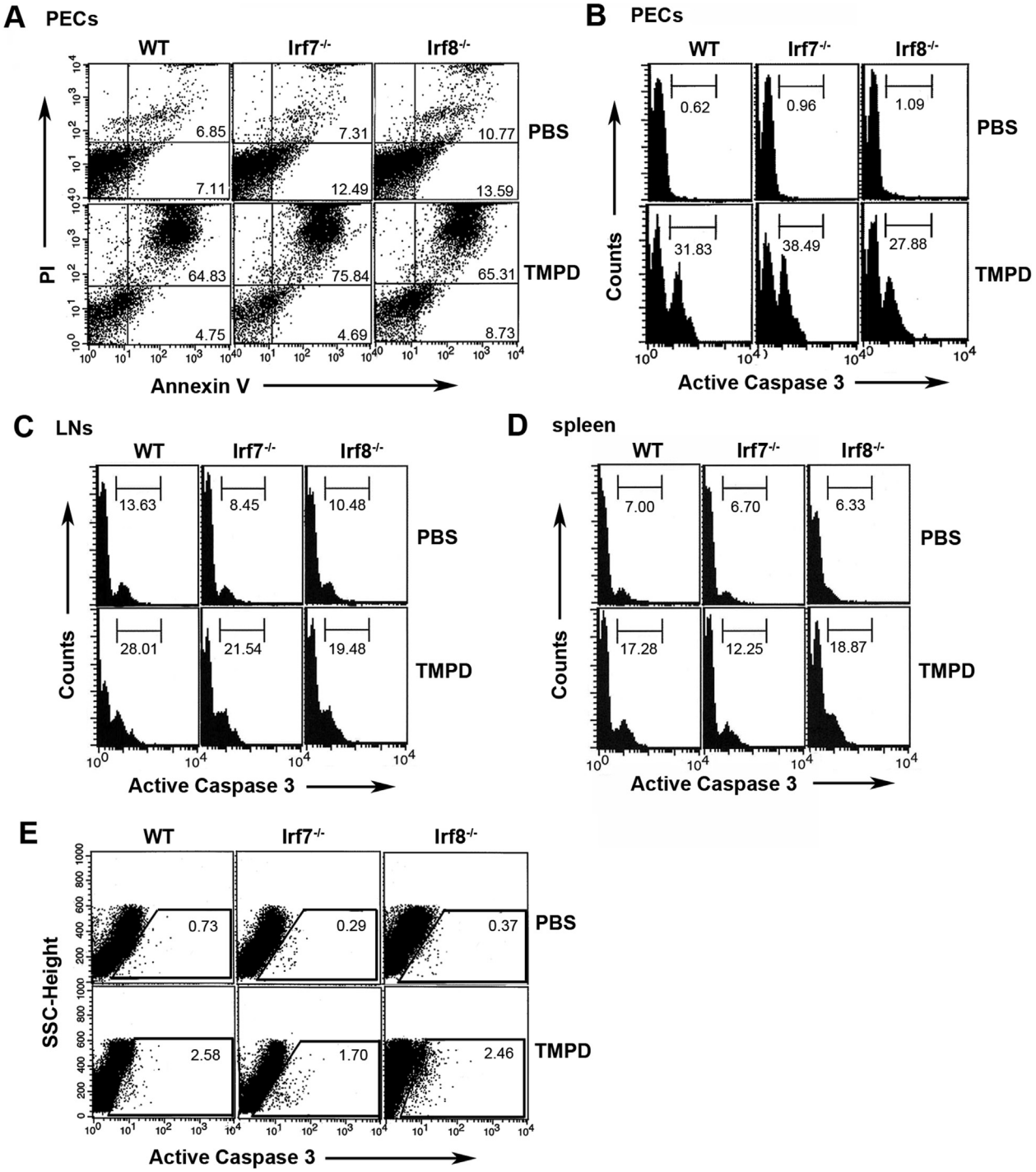

Fig. 3. TMPD induced apoptosis. (A, B) PECs were freshly isolated from WT, *Irf7*$^{-/-}$, and *Irf8*$^{-/-}$ mice and cultured *ex vivo* with 75 μM TMPD/β -CyD. After 16 h, the cells were harvested, stained with FITC-annexin V/propidium iodide (A), anti-active caspase-3 Ab (B), and analyzed by flow cytometry. The cells from all strains went into apoptosis in the presence of TMPD. Numbers indicate positive cells. One representative result of three is shown. (C, D) Inguinal LNs (C) and spleens (D) were freshly isolated from three strains, cultured *ex vivo* with 150 μM TMPD/β-CyD, for 16 h and stained with anti-active caspase-3 Ab as above. Numbers in histograms indicate percentage of active caspase 3-expressing cells. One representative result of three is shown. (E) PECs were harvested 2 weeks after TMPD or PBS injection and stained with anti-active caspase-3Ab. The percentage of active caspase 3-expressing cells is indicated. Data are representative of three independent experiments.

through the production of proinflammatory cytokines (or IFNs). One of the pathogenic mechanisms by which TMPD challenge causes SLE in mice has been linked to the induction of Ly6C^{high} monocytes in the peritoneal cavity [10]. Ly6C^{high} monocytes are termed inflammatory monocytes because of their quick recruitment to the site of inflammation or infection [17]. Ly6C^{high} monocytes, but not plasmacytoid DCs (pDCs), are a major source of type I IFN in this experimental model [10]. These monocytes persist for ~3 days before undergoing a programmed cell death (apoptosis) [15]. We examined PECs for the presence of Ly6C^{high} monocytes 2 weeks following the TMPD injection an all mouse strains. As shown in Fig. 4A, the influx of Ly6C^{high}CD11b^{+}Ly6G^{-} inflammatory monocytes into the peritoneal cavity was strongly induced in WT and *Irf7*$^{-/-}$ mice but not in *Irf8*$^{-/-}$ mice. Ly6C^{high} monocytes do not persistently exist in the peritoneal cavity. However, they become ~30% of PECs two weeks after the TMPD injection through homing facilitated by CCL2. The IRF8-KLF4 axis is a crucial component of the monocyte differentiation, which explains the lack of Ly6C^{high} monocytes in *Irf8*$^{-/-}$ mice [18].

The analysis of the peritoneal infiltrate at various time points after TMPD challenge revealed that inflammatory monocytes accumulated in the peritoneal cavity constituting ~30% of PECs throughout the course (Fig. 4B and C). These inflammatory monocytes appeared in the peritoneal cavity one day after i.p. injection of TMPD and persisted for several months afterwards in both WT and *Irf7*$^{-/-}$ mice. They were completely absent in *Irf8*$^{-/-}$ mice throughout all the time points tested (Fig. 4B and C). Ly6C^{high}CD11b^{+}Ly6G^{-} inflammatory monocytes were almost negative for CD11c and about 15% of the cells expressed MHC class II (Fig. 4D).

We also found that the infiltrate of inflammatory monocytes was observed in kidney in WT and *Irf7*$^{-/-}$ mice but not in *Irf8*$^{-/-}$ mice (Fig. 4E and F). Since an influx of monocytes supposedly plays a significant role in the pathogenesis of human and murine lupus nephritis [19], these results suggest that the inflammatory monocytes recruited to the kidney might be responsible for the renal damage in WT and *Irf7*$^{-/-}$ mice.

To assess their functional nature, we next examined cytokine production from Ly6C^{high}CD11b^{+}Ly6G^{-} inflammatory monocytes. They mildly produced proinflammatory cytokines such as IL-6, TNF-α, IL-1α, and IL-1β which were markedly increased in response to dsDNA autoantigen in WT and *Irf7*$^{-/-}$ mice (Fig. 5A). Consistent with this, serum levels of TNF-α and IL-6 showed similar increase in WT and *Irf7*$^{-/-}$ mice but were decreased in *Irf8*$^{-/-}$ mice following the TMPD challenge (Fig. 5B) [9].

3.5. Loss of IFN signature in TMPD-treated *Irf7*$^{-/-}$ and *Irf8*$^{-/-}$ mice

Since signaling of type I IFN is recognized as central to the pathogenesis of SLE [20], it is possible that type I IFN signaling is deficient in *Irf7*$^{-/-}$ and *Irf8*$^{-/-}$ mice. We thus examined if ISGs such as Mx-1 and IRF7 are induced in our model mice 2 weeks after the TMPD challenge. Real-time PCR revealed that expressions of Mx-1, a specific sensor of interferon levels, and IRF7 were diminished in PECs from *Irf7*$^{-/-}$ and *Irf8*$^{-/-}$ mice while they were greatly enhanced in WT mice (Fig. 5C) [9]. To examine the role of Ly6C^{high} inflammatory monocytes in this context, we next determined the expression of ISGs in these cells as Ly6C^{high} inflammatory monocytes are considered to be the major source of type I IFN in this model [10]. Curiously, Mx-1 and IRF7 were not detectable in TMPD-treated *Irf7*$^{-/-}$ mice (Fig. 5D), providing an explanation for the lack of the autoantibody production in these mice. These results validate our hypothesis that type I IFN production by Ly6C^{high} monocytes play a major role in the development of SLE in mice following the TMPD challenge.

3.6. Ly6C^{high} inflammatory monocytes give rise to dendritic cells

The lack of the development of autoimmunity in *Irf7*$^{-/-}$ and *Irf8*$^{-/-}$ mice following the TMPD challenge may also involve the diminished presentation of autoantigens to T cells. Therefore, we asked if Ly6C^{high} monocytes efficiently differentiate into DCs in these mice, in light of previous literature suggesting that sera from SLE patients contain factors including IFN-α that induce monocytes to differentiate into DCs, which then capture antigens from apoptosed cells and present to CD4 T cells as antigen presenting cells [21]. Since inflammatory monocytes can differentiate into inflammatory DCs in tissues [17,22], we determined if Ly6C^{high}CD11b^{+}Ly6G^{-} monocytes accumulating in the peritoneal cavity could efficiently differentiate into functional DCs in our model of SLE. Ly6C^{high}CD11b^{+}Ly6G^{-} monocytes were sorted from the peritoneal cavity of WT mice two weeks after the injection of TMPD (Fig. 6A) and their expression of DC markers was first examined. To strictly study the *in vivo* commitment of inflammatory monocytes into DCs under the current environment, we adoptively transferred sorted Ly6C^{high}CD11b^{+}Ly6G^{-} inflammatory monocytes from CD45.1 mice into congenic CD45.2^{+}WT hosts. Only cells that were negative for CD11c were sorted and transferred into CD45.2^{+}WT mice that have pre-treated with TMPD two weeks prior to the transfer. As shown in Fig. 6B, CD45.1^{+}Ly6C^{high} monocytes migrated from the peritoneal cavity to the spleen in host mice. As described above, the sorted CD45.1 inflammatory monocytes were CD11c negative at the time of transfer. Curiously, donor-derived monocytes in the host spleen showed enhanced expression of CD11c one week after the adoptive transfer, and approximately 10% of donor-derived monocytes expressed both CD11c and MHC class II, indicative of the differentiation *in vivo* of monocytes to DCs (Fig. 6B and C). Using *Irf7*$^{-/-}$ congenic donor and host, we observed that the differentiation of Ly6C^{high}CD11b^{+}Ly6G^{-} monocytes into CD11c^{+}DCs occur in the absence of IRF7 (Fig. 6C, Supplementary Fig. 2A). Moreover, cross-over approach by the transfer of inflammatory monocytes from WT and Irf7$^{-/-}$ mice into the irrelevant host (Irf7$^{-/-}$ and WT, respectively) showed differentiation into DCs in both cases, indicating this effect is cell-intrinsic (Fig. 6C, Supplementary Fig. 2B and C).

Double immunofluorescence staining confirmed the presence of donor-derived CD11c^{+} cells in the spleen of host mice (Fig. 6D, Supplementary Fig. 2D). It appeared that donor-derived DCs formed clusters in the host spleen and resided in a location that is different from the one for host-derived DCs (Fig. 6D, Supplementary Fig. 2D).

3.7. Inflammatory monocyte-derived DCs respond to dsDNA and produce proinflammatory cytokines

We next tested if DCs differentiated from inflammatory monocytes were functionally competent in that they have the capacity to produce proinflammatory cytokines in response to dsDNA antigen. Sort-purified Ly6C^{high}CD11b^{+}Ly6G^{-} inflammatory monocytes were adoptively transferred and the spleen of a host was examined by intracellular cytokine staining for the presence of cytokine-producing DCs. Inflammatory monocyte-derived DCs from CD45.1^{+}WT mice showed discernible production of TNF-α, IL-1α, and IL-1β, but not IL-6 in response to dsDNA antigen (Fig. 7A). Donor-derived DCs produced similar amount of TNF-α, IL-1α, and IL-1β in the absence of IRF7 (Fig. 7B). Similarly, donor-derived DCs transferred into the irrelevant host also produced proinflammatory cytokines, indicating they were functional (Fig. 7C and D).

4. Discussion

In our previous report studying *Irf7*$^{-/-}$ mice, we demonstrated that the two major disease manifestations of SLE, the autoantibody production and the glomerulonephritis can be uncoupled because they are mediated by distinct molecular mechanisms. In this report, we studied the relevant mechanisms responsible for the SLE development in our model and demonstrated that the development and homing of inflammatory monocytes/monocyte-derived DCs control the onset of SLE under the influence of another interferon regulatory factor, IRF8. TMPD, which triggers SLE in our model, induces the homing of DC subset to the spleen

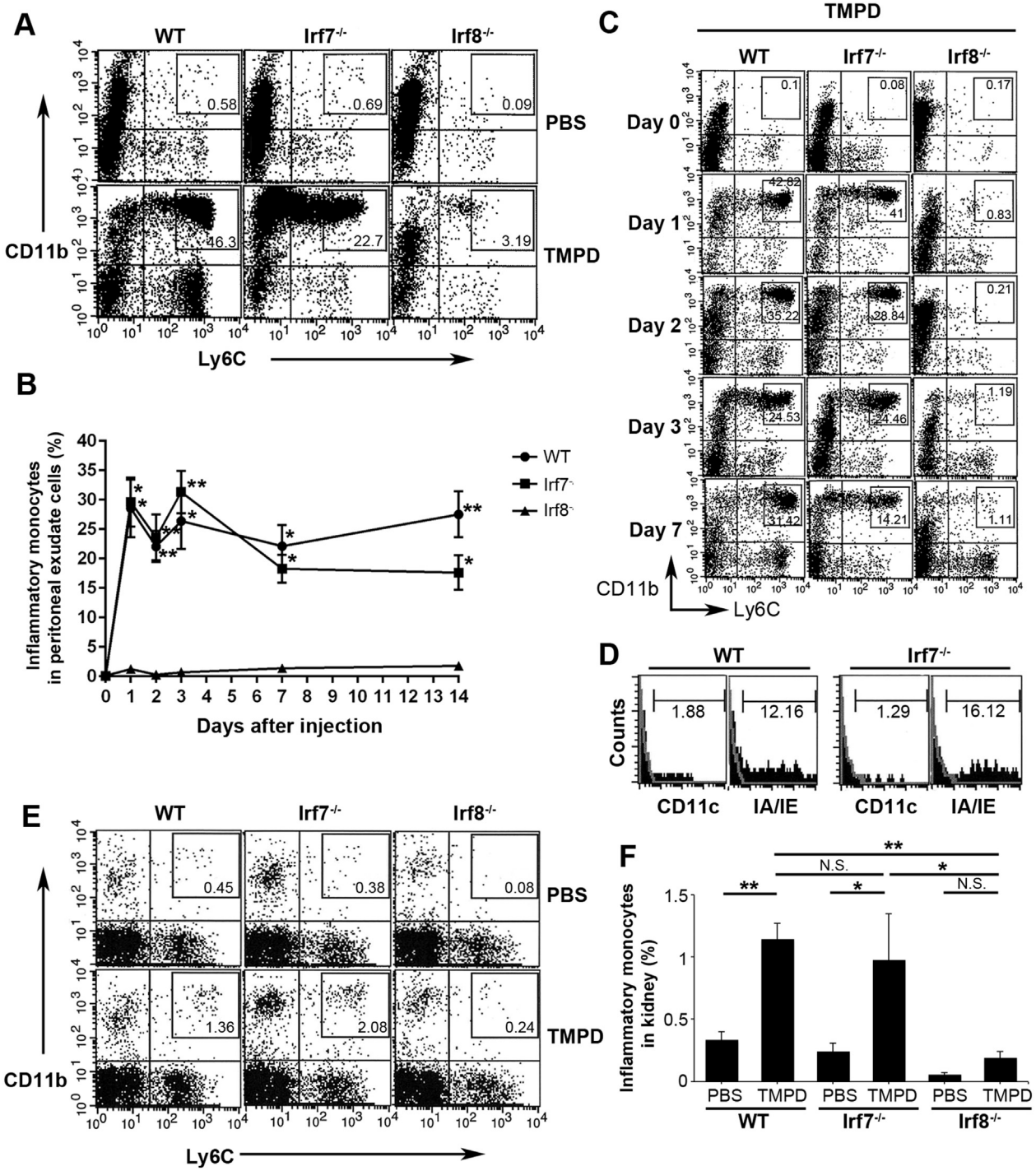

Fig. 4. Recruitment of Ly6C^{high} monocytes in WT and *Irf7*$^{-/-}$ mice. (A, B) Flow cytometric analysis of PECs 2 weeks after TMPD injection. TMPD was injected into three strains and PECs were analyzed for inflammatory monocyte (CD11b^{+}Ly6C^{high}Ly6G^{-}) by flow cytometry. A dramatic expansion of inflammatory monocyte was observed following the TMPD treatment in WT and *Irf7*$^{-/-}$ mice but not in *Irf8*$^{-/-}$ mice. Cells were first gated on the lymphocyte population and then gated out Ly6G^{+} cells. (A) Representative flow cytometric analysis is shown. The percentage of inflammatory monocytes is indicated. Data are representative of at least five independent experiments. (B) Dynamics of cellular infiltrate in PECs after TMPD administration. The average percentage of CD11b^{+}Ly6C^{high}Ly6G^{-} cells from the peritoneal cavity at indicated time points after TMPD injection was shown (n = 3–9 mice/group). Error bars represent SEM. *; $p < 0.05$ and **; $p < 0.01$ vs *Irf8*$^{-/-}$. One-way ANOVA with Tukey HSD test. (C) Representative flow cytometric plots of (B) at the indicated time points after TMPD injection are shown. (D) PECs were analyzed for the expression of CD11c and MHC class II 2 weeks after the TMPD injection. The percentages of CD11b^{+}Ly6C^{high}Ly6G^{-} cells expressing CD11c or MHC class II are indicated. Cells were first gated on the lymphocyte population, gated out Ly6G^{+} cells, and then gated on CD11b^{+}Ly6C^{high} cells. One representative dot plot of three experiments is shown. The thin line represents isotype control staining. (E) Flow cytometric analysis of single cell suspension from kidneys 2 weeks after the TMPD injection. The TMPD challenge induced the infiltration of inflammatory monocytes (CD11b^{+}Ly6C^{high}Ly6G^{-}) in WT and *Irf7*$^{-/-}$ mice but not in *Irf8*$^{-/-}$ mice. The percentages of inflammatory monocytes are indicated. One representative result of three is shown. (F) The percentage of inflammatory monocytes in kidney was determined by flow cytometry and the average percentage from n = 3–5 mice per group is shown (error bars, SEM). *; $p < 0.05$ and **; $p < 0.01$ by one-way ANOVA with Tukey HSD test. N.S. not significant.

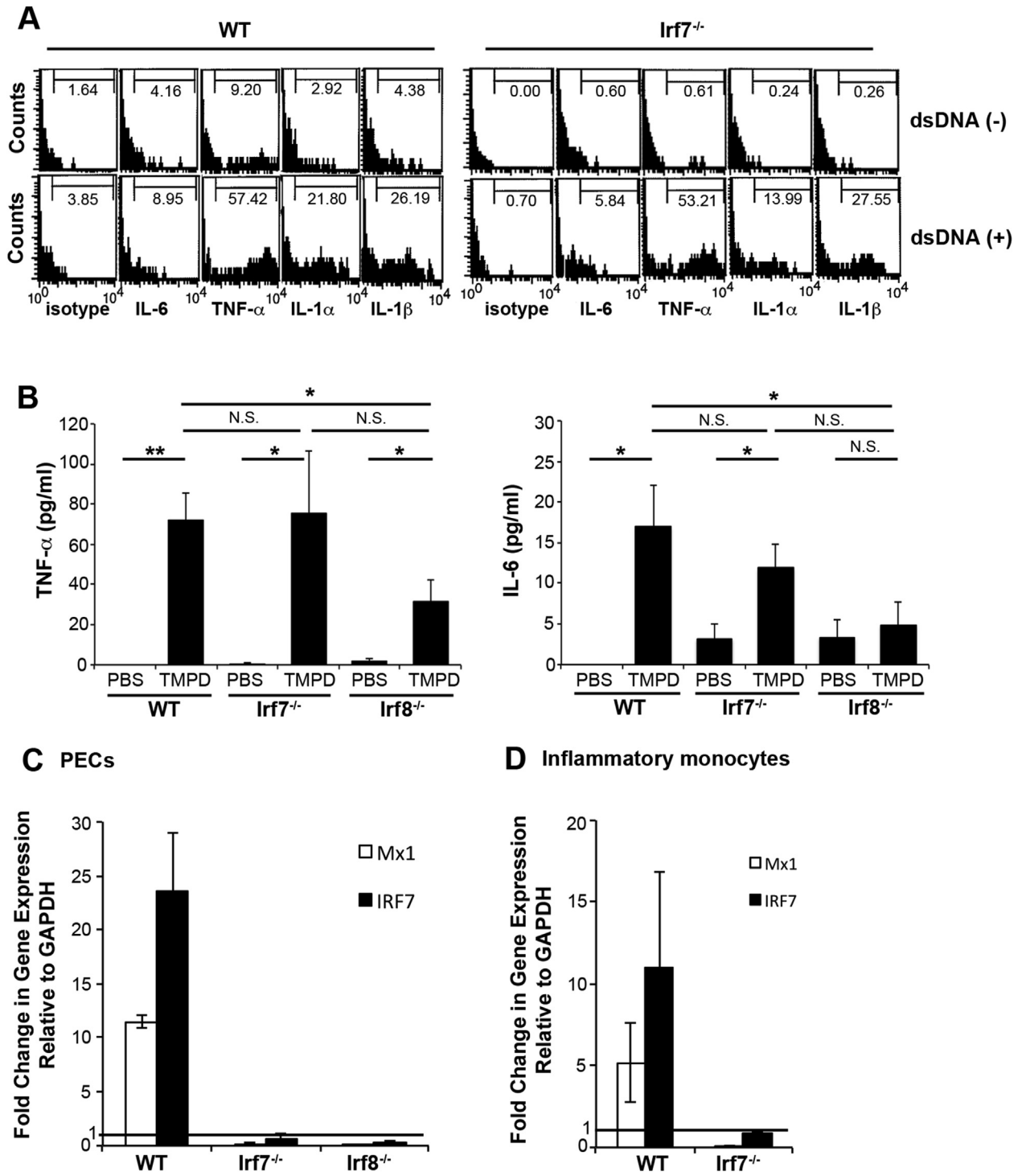

Fig. 5. Production of proinflammatory cytokines, but not that of type I IFN, in the absence of IRF7 by inflammatory monocytes.(A) Intracellular stainings for proinflammatory cytokines were performed on PECs after incubation with or without dsDNA. Stainings of Ly6C^{high}CD11b^{+}Ly6G^{-} cells within the lymphocyte gate are shown. Percentages of Ly6C^{high}CD11b^{+}Ly6G^{-} cells producing indicated cytokines are indicated. Data are representative of three independent experiments. (B) Serum levels of TNF-α and IL-6 were determined by ELISA 2 weeks after PBS or TMPD injection. Almost similar increase of serum TNF-α and IL-6 was observed in sera from WT and Irf7$^{-/-}$ mice after TMPD injection. In contrast, serum levels of these cytokines were decreased in TMPD-treated *Irf8*$^{-/-}$ mice. Data are representative of two independent experiments (n = 9–15 mice per group). Error bars = SEM. *; $p < 0.05$ and **; $p < 0.01$ by one-way ANOVA with Tukey HSD test. N.S. not significant. (C) Expression of the ISGs (MX1 and IRF7) in PECs as determined by real-time PCR. PECs were isolated 2wk after PBS or TMPD injection. The data were normalized to GAPDH and fold change in reference to PBS-treated WT, Irf7$^{-/-}$, or Irf8$^{-/-}$ mice are shown. Expression of ISGs was only detected in PECs from WT mice. Data were pooled from two independent experiments with triplicates in each experiment. Error bars = SEM. (D) Profound decrease of the expression of the ISGs in the absence of IRF7 by purified inflammatory monocytes. Gene expression was measured from purified monocytes 2 weeks after TMPD injection. Fold changes in reference to PECs from PBS-treated WT and Irf7$^{-/-}$ mice, respectively are shown. Expression of ISGs was detected in only purified inflammatory monocytes from WT mice. Data were pooled from two independent experiments with triplicates in each experiment. Error bars = SEM.

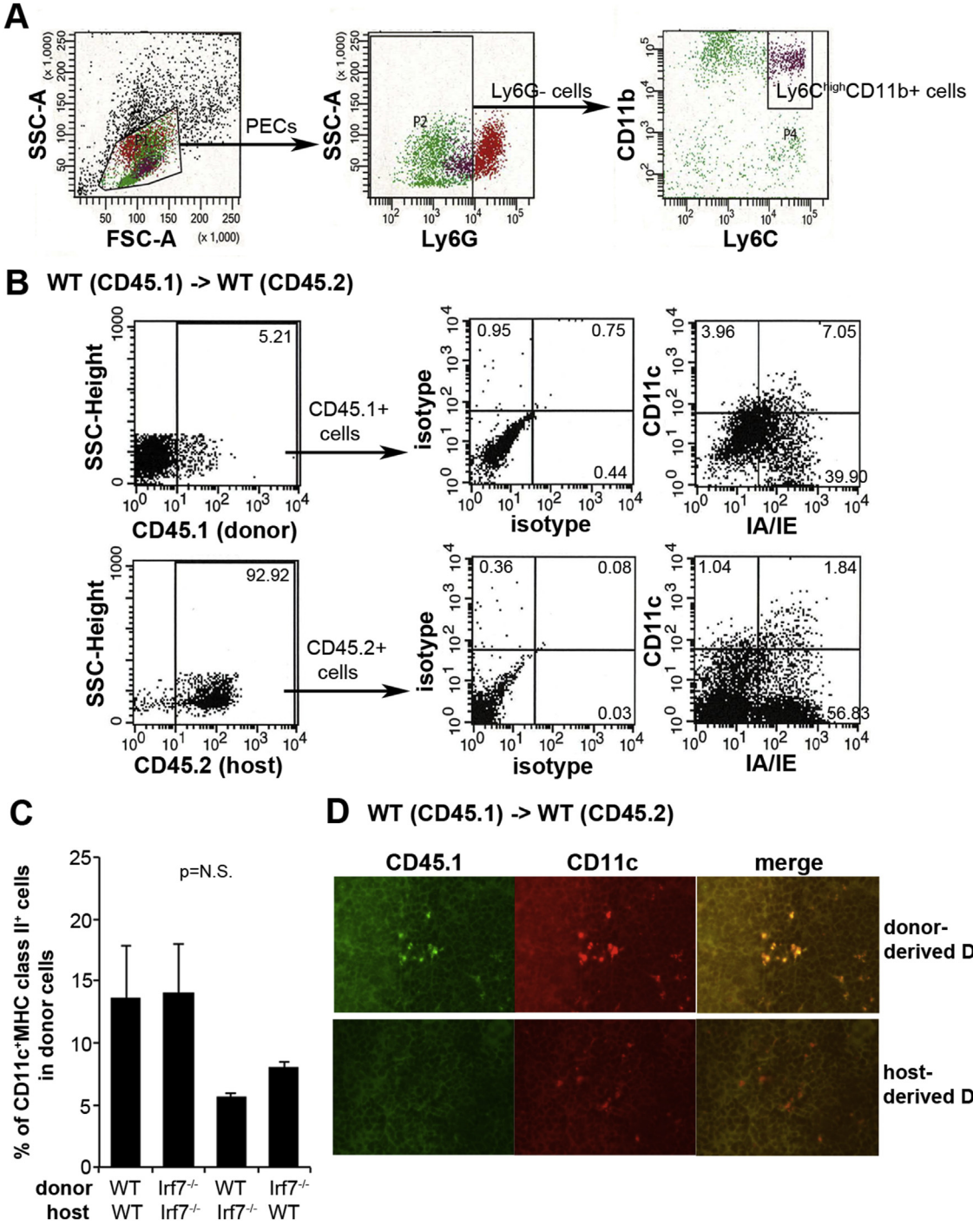
A
SSC-A
FSC-A
PECs
Ly6G- cells
Ly6G
CD11b
Ly6C
Ly6C^high CD11b+ cells
B WT (CD45.1) -> WT (CD45.2)
SSC-Height
CD45.1 (donor)
5.21
CD45.1+ cells
isotype
0.95
0.75
0.44
CD11c
IA/IE
3.96
7.05
39.90
CD45.2 (host)
92.92
CD45.2+ cells
0.36
0.08
0.03
1.04
1.84
56.83
C
% of CD11c+MHC class II+ cells in donor cells
p=N.S.
donor WT Irf7-/- WT Irf7-/-
host WT Irf7-/- Irf7-/- WT
D WT (CD45.1) -> WT (CD45.2)
CD45.1
CD11c
merge
donor-derived DC
host-derived DC

Fig. 6. Differentiation of DCs from inflammatory monocytes. (A) Gating strategy for FACS-sorting. Representative flow cytometry profiles of PECs prepared from CD45.1 congenic mice treated with TMPD 2 weeks previously, showing gating strategy used for FACS-sorting. PECs were gated based on FSC and SSC, and Ly6G$^+$ cells were excluded. Ly6C^{high} CD11b$^+$ inflammatory monocytes were then gated based on Ly6C and CD11b expression and sorted. (B) Flow cytometric analysis of the spleen from TMPD-challenged CD45.2$^+$WT mouse (host) injected with CD45.1$^+$ inflammatory monocytes sorted from CD45.1$^+$WT mice (donor). The sorted CD45.1$^+$inflammatory monocytes were injected into CD45.2$^+$ WT host mouse on day 14 after the TMPD challenge and the spleen of the host was harvested 6 days later. The spleen from the CD45.2$^+$ WT host was analyzed by flow cytometry. Some of the donor-derived CD45.1$^+$inflammatory monocytes expressed CD11c and MHC class II (upper panels). The host-derived CD45.2$^+$DCs expressing CD11c and MHC class II were also present in the spleen (lower panels). The dot plot graphs were created by gating on CD45.1$^+$ cells (upper panels) or CD45.2$^+$ cells (lower panels) within the lymphocyte gate. The numbers in the dot plot graphs indicate positive cells. One representative dot plot of six experiments was shown. (C) The percentages of CD11c$^+$MHC class II$^+$ cells among transferred donor cells in the spleens of the host mice are shown. Inflammatory monocytes were sorted from the indicated donor mice and transferred into the indicated host mice as described in (B). CD45.1$^+$WT, CD45.1$^+$Irf7$^{-/-}$, CD45.1$^+$WT, and CD45.2$^+$Irf7$^{-/-}$ mice were used as donors and CD45.2$^+$WT, CD45.2$^+$Irf7$^{-/-}$, CD45.2$^+$Irf7$^{-/-}$, and CD45.1$^+$WT mice were used as hosts, respectively. The spleen from the host was analyzed by flow cytometry. The dot plot graphs were created by gating on CD45.1$^+$ cells (for donor mice; CD45.1$^+$WT, CD45.1$^+$Irf7$^{-/-}$, CD45.1$^+$WT) or CD45.2$^+$ cells (for donor mice; CD45.2$^+$Irf7$^{-/-}$) within the lymphocyte gate and the percentage of IA/IE$^+$CD11c$^+$ double-positive cells were determined. The average percentage of 3–5 host mice per group is shown. Error bars represent SEM. *$0.01 < p < 0.05$. Data were pooled from three to five independent experiments. N.S. not significant by one-way ANOVA with Tukey HSD test. (D) Immunofluorescence staining of frozen section from the spleen of the CD45.2$^+$WT host mouse for the identification of CD11c-expressing CD45.1$^+$ cells. The sorted inflammatory monocytes from CD45.1$^+$WT donor mice were injected into CD45.2$^+$ WT host mouse on day 14 after the TMPD challenge and the spleen of the host mouse was harvested 6 days later. The spleen from CD45.2$^+$WT host mouse was stained with FITC-CD45.1 A b and PE-CD11c Ab. The donor-derived CD45.1$^+$ cells (green) expressed CD11c (red) (upper panels). In comparison, the host-derived DC in the same slide was CD45.1 negative and CD11c positive (lower panels). The One representative image of three experiments was shown. . (For interpretation of the references to colour in this figure legend, the reader is referred to the Web version of this article.)

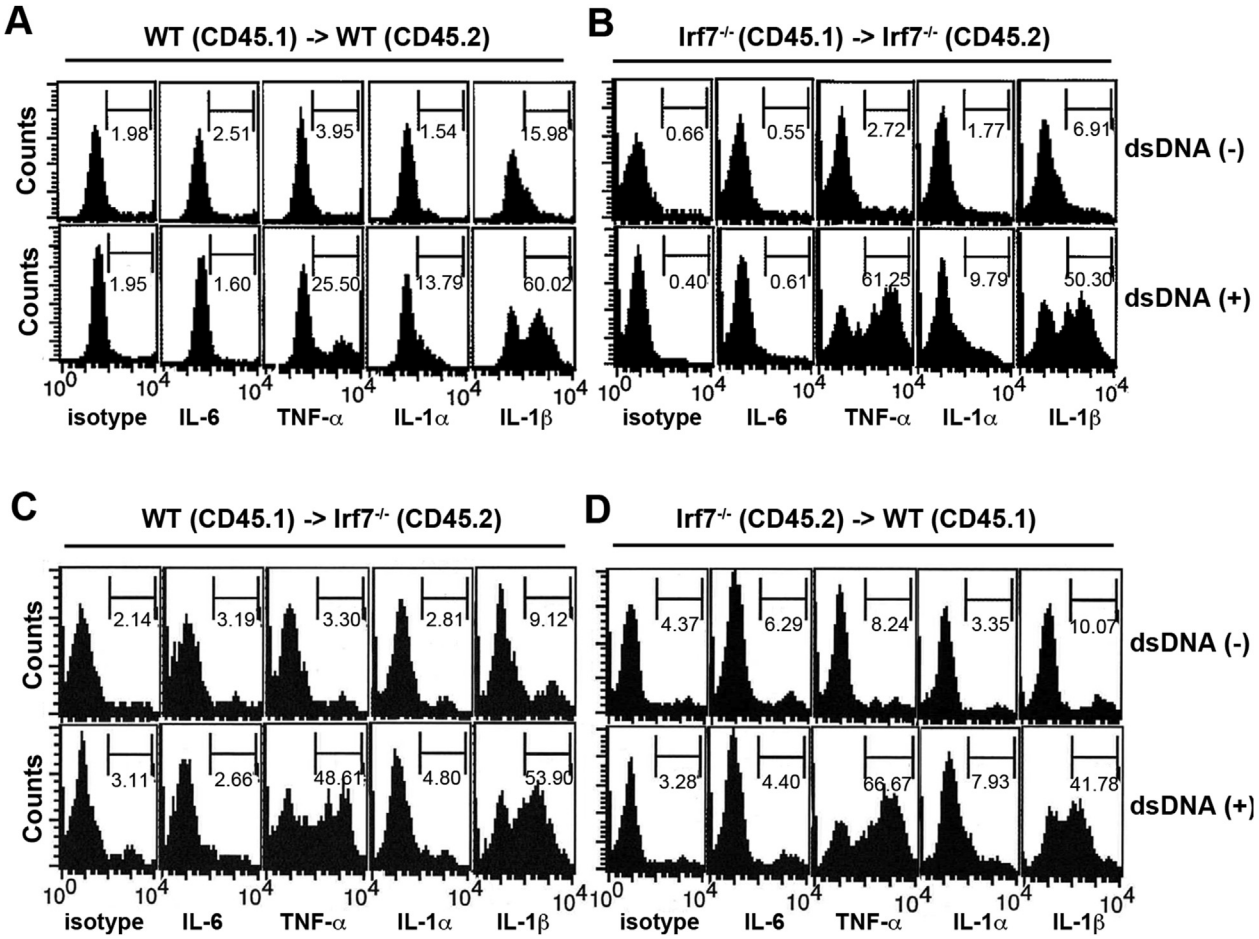

Fig. 7. Inflammatory monocytes derived-DCs produced proinflammatory cytokines in response to dsDNA. (A–D) The spleen from the host was subjected to intracellular staining for proinflammatory cytokines after incubation with or without dsDNA. Inflammatory monocytes were sorted from the indicated donor mice and transferred into the indicated host mice on day 14 after the TMPD challenge. The spleen of the host was harvested 6 days later and analyzed by flow cytometry. The combination of donor and host mice (donor - > host) was indicated above the line of each panel. Cells were gated on donor-derived CD11c$^+$ cells (A-C; CD45.1$^+$CD11c$^+$ cells, D; CD45.2$^+$CD11c$^+$ cells) within the lymphocyte gate. The percentage of donor-derived CD11c$^+$ cells producing indicated cytokines is indicated. One representative dot plot of three experiments each was shown.

following its differentiation from inflammatory monocytes in the peritoneal cavity. Production by DCs of type I IFN and proinflammatory cytokines in response to dsDNA is critical for the SLE development.

During inflammation or infection, a certain type of blood monocytes gives rise to populations of inflammatory DCs [17]. These monocytes, originated from the bone marrow with Gr1$^+$Ly6C$^+$Ly6G$^-$F4/8$^+$CD11b$^+$CD11c$^-$ phenotype, were termed inflammatory monocytes because they are selectively recruited to the site

of infection and inflammation in a CCR2-dependent fashion [17,23–25]. Once within the tissue, inflammatory monocytes would differentiate into inflammatory DCs such as TNF/iNOS-producing DCs (TipDCs) which then migrate to the LNs and the white pulp of the spleen where they interact with T cells and stimulate them [17,22]. These monocyte-derived DCs mediate innate defense against intracellular bacterial pathogens and have critical roles in the eradication of bacteria [23]. In humans, TipDC robustly expand in skin lesions of psoriasis, suggesting their role as a major inflammatory and effector cells in psoriasis [26]. However, the role of inflammatory monocyte-derived DCs in autoimmunity has not been well understood. Our report thus makes one of the pioneering studies in this context.

The type I IFN pathway plays a pivotal etiopathogenic role in SLE [27–29]. Increased serum levels of type I IFN [30] and the subsequent enhancement of the ISG expression (IFN signature) in peripheral blood mononuclear cells [31,32] are prominent features in SLE patients. Consistent with this, IFN-I receptor α-chain-deficient mice (*Ifnar*$^{-/-}$ mice) failed to develop SLE with no production of autoantibodies nor the development of glomerulonephritis upon TMPD challenge [20]. Both *in vivo* [33] and *in vitro* [34] studies support that the hyperproduction of type I IFNs from pDCs is critical for the pathogenesis of lupus. TMPD-induced lupus model exhibits a robust IFN signature that recapitulates the IFN signature in human SLE patients and might therefore be a useful model for the study of IFN-dysregulation in SLE [15,35]. We also note the limitation of it that IFN-producing cells of this model are somewhat different from those in other lupus models and human SLE patients as reported [15,33–35]. Using this model, we previously revealed a novel role for IRF7 in the pathogenesis of SLE [9] as described above. We demonstrated that the two signature facets of SLE, the production of the autoantibody and the development of glomerulonephritis are molecularly independent. We proposed that the type I IFN pathway (IRF7 dependent) is critical for the autoantibody production whereas the NF-κB activation (IRF7 independent) sufficiently enables the development of glomerulonephritis. To further advance our understanding, we hereby tested *Irf8*$^{-/-}$ mice because IRF8 regulates both type I IFN and NF-κB pathways. Furthermore, we sought after the source of proinflammatory cytokines and type I IFN and identified inflammatory monocytes/monocyte-derived DCs as their source. We demonstrated that inflammatory monocytes and monocyte-derived DCs were recruited and produced proinflammatory cytokines but failed to produce type I IFN in the absence of IRF7, accounting for the discordance of the two major SLE events described above [9]. Our current study validates that proinflammatory cytokines induced by autoantigen stimulation augment local proinflammatory effects independent of the autoantibody production. It also demonstrates that the recruitment of inflammatory monocytes/monocyte-derived DCs is dependent on IRF8. Therefore, TMPD failed to induce either the autoantibody production or the development of glomerulonephritis in the absence of IRF8.

It is well described that IRF7 is critical for the induction of type I IFN mediated by pattern-recognition receptors (PRRs) including endogenous TLRs (TLR7 and TLR9) [5,36] as Irf7$^{-/-}$ mice are vulnerable to viral infection because they are unable to produce IFN-α [5]. While IRF8 can also contribute to type I IFN induction, the effect of IRF8 on cytokines is limited and IRF8 plays a broader role in immune system and normal hematopoiesis. IRF8 is required for the development of monocytes, macrophages, DCs, basophils and eosinophils, while it inhibits the generation of neutrophils [37]. As such, IRF8-deficiency has been shown to result in animals lacking pDCs [38], CD8α^{+}DCs [39], much reduced levels of monocytes [13,40] and expanded levels of granulocytes [13], abnormal germinal center B cell function due to modulated BCL6/AICDA expression [41].

A role for IRF8 in the pathogenesis of SLE was previously demonstrated using IRF8-deficient NZB mice which are deficient in pDCs. These mice show almost complete absence of autoantibodies, along with reduced kidney disease [33]. These effects were observed despite normal B-cell responses to TLR7 and TLR9 stimuli and intact humoral responses to conventional T-dependent and -independent antigens. The report concluded that pDCs and the production of type I IFNs by these cells are critical contributors to the pathogenesis of lupus-like autoimmunity in these models. However, we argue that the role of pDCs might be limited in the TMPD-induced lupus despite the current belief that they are the primary source of type I IFN in both healthy individuals and SLE patients, because the depletion of pDCs showed little effects on type I IFN or ISG expression in TMPD-induced lupus mouse models [10,15]. In contrast, inflammatory monocytes that accumulate in the inflamed peritoneum of these mice may be the major source of type I IFN because their depletion with clodronate-containing liposomes rapidly eliminated the expression of type I IFN and ISGs [10]. Curiously, the recruitment of Ly6C^{high} inflammatory monocytes into the peritoneum was abolished in type I IFN receptor-deficient mice but was unaffected by the absence of IFN-γ, TNF-α, IL-6, or IL-1 [42].

While we were preparing this manuscript, a similar work on TMPD-induced lupus mouse model using Irf8$^{-/-}$ mice came out although they focused on a pathological role of inflammatory monocytes in diffuse alveolar hemorrhage [43]. They demonstrated that the infiltration of Ly6C^{high} monocytes and the upregulation of IFN-inducible genes were diminished in the absence of Irf8. They also demonstrated that hypergammaglobulinemia, ANAs, anti-U1RNP Abs, and glomerulonephritis were all markedly reduced in Irf8$^{-/-}$ mice after TMPD treatment [43]. These data are consistent with our data. However, our study added unique findings that inflammatory monocytes further differentiated into DC and could respond to autoantigen.

Taken together, we demonstrated that proinflammatory cytokines produced from inflammatory monocyte/monocyte-derived DCs were involved in tissue damage of SLE in WT and *Irf7*$^{-/-}$ mice independent of autoantibody production and that type I IFN from those cells contributes to the autoantibody production. Since type I IFN induces maturation and activation of DCs [44], results from the present study suggest that the loss of type I IFN production as observed in *Irf7*$^{-/-}$ and *Irf8*$^{-/-}$ mice might affect antigen presentation. These impairments in antigen presentation and less activation of CD4 T cells as observed in *Irf7*$^{-/-}$ mice ultimately inhibit the autoantibody production.

Our observation suggests unique roles for IRF7 and IRF8 in their distinct contribution to the pathogenesis of SLE. The translational explanation of this study might help develop novel therapeutic strategies for SLE by targeting these factors and inflammatory monocytes/dendritic cells.

Author contributions

FM conceived, performed experiments, and analyzed data. FM, YT, KO designed the study. KH contributed to the sorting experiments. FM, YT wrote the manuscript with all authors contributing to writing.

Declaration of competing interest

The authors declare no conflict of interest.

Acknowledgments

We thank Ayako Yamamoto for technical assistance.

This work was supported in part by Japan Society for the Promotion of Science Grants-in-Aid for Scientific Research (15K09779 and 19K08797 to F.M.), by a research grant from the Lydia O'Leary Memorial Pias Dermatological Foundation (to F.M.), Novartis Research Grants (to F.M.), and a research grant from Sanofi (to F.M. and H.A.)

Appendix A. Supplementary data

Supplementary data to this article can be found online at https://doi.org/10.1016/j.jtauto.2020.100060.

References

[1] Z. Liu, A. Davidson, Taming lupus-a new understanding of pathogenesis is leading to clinical advances, Nat. Med. 18 (2012) 871–882.
[2] G.C. Tsokos, M.S. Lo, P. Costa Reis, K.E. Sullivan, New insights into the immunopathogenesis of systemic lupus erythematosus, Nat. Rev. Rheumatol. 12 (2016) 716–730.
[3] J. Bentham, D.L. Morris, D.S.C. Graham, C.L. Pinder, P. Tombleson, T.W. Behrens, et al., Genetic association analyses implicate aberrant regulation of innate and adaptive immunity genes in the pathogenesis of systemic lupus erythematosus, Nat. Genet. 47 (2015) 1457–1464.
[4] T. Tamura, H. Yanai, D. Savitsky, T. Taniguchi, The IRF family transcription factors in immunity and oncogenesis, Annu. Rev. Immunol. 26 (2008) 535–584.
[5] K. Honda, H. Yanai, H. Negishi, M. Asagiri, M. Sato, T. Mizutani, et al., IRF-7 is the master regulator of type-I interferon-dependent immune responses, Nature 434 (2005) 772–777.
[6] L. Gabriele, K. Ozato, The role of the interferon regulatory factor (IRF) family in dendritic cell development and function, Cytokine Growth Factor Rev. 18 (2007) 503–510.
[7] X. Ouyang, R. Zhang, J. Yang, Q. Li, L. Qin, C. Zhu, et al., Transcription factor IRF8 directs a silencing programme for TH17 cell differentiation, Nat. Commun. 2 (2011) 314.
[8] F. Miyagawa, H. Zhang, A. Terunuma, K. Ozato, Y. Tagaya, S.I. Katz, Interferon regulatory factor 8 integrates T-cell receptor and cytokine-signaling pathways and drives effector differentiation of CD8 T cells, Proc. Natl. Acad. Sci. U.S.A. 109 (2012) 12123–12128.
[9] F. Miyagawa, Y. Tagaya, K. Ozato, H. Asada, Essential requirement for IFN regulatory factor 7 in autoantibody production but not development of nephritis in murine lupus, J. Immunol. 197 (2016) 2167–2176.
[10] P.Y. Lee Py, J.S. Weinstein, D.C. Nacionales, P.O. Scumpia, Y. Li, E. Butfiloski, et al., A novel type I IFN-producing cell subset in murine lupus, J. Immunol. 180 (2008) 5101–5108.
[11] L. Bossaller, A. Christ, K. Pelka, K. Nundel, P.I. Chiang, C. Pang, et al., TLR9 deficiency leads to accelerated renal disease and myeloid lineage abnormalities in pristane-induced murine lupus, J. Immunol. 197 (2016) 1044–1053.
[12] A.J. Swaak, J.C. Nossent, W. Bronsveld, A. van Rooyen, E.L. Nieuwenhuys, L. Theuns, et al., Systemic lupus erythematosus. II. Observations on the occurrence of exacerbations in the disease course: Dutch experience with 110 patients studied prospectively, Ann. Rheum. Dis. 48 (1989) 455–460.
[13] T. Holtschke, J. Lohler, Y. Kanno, T. Fehr, N. Giese, F. Rosenbauer, et al., Immunodeficiency and chronic myelogenous leukemia-like syndrome in mice with a targeted mutation of the ICSBP gene, Cell 87 (1996) 307–317.
[14] D.C. Nacionales, K.M. Kelly, P.Y. Lee, H. Zhuang, Y. Li, J.S. Weinstein, et al., Type I interferon production by tertiary lymphoid tissue developing in response to 2,6,10,14-tetramethyl-pentadecane (pristane), Am. J. Pathol. 168 (2006) 1227–1240.
[15] W.H. Reeves, P.Y. Lee, J.S. Weinstein, M. Satoh, L. Lu, Induction of autoimmunity by pristane and other naturally occurring hydrocarbons, Trends Immunol. 30 (2009) 455–464.
[16] N. Calvani, R. Caricchio, M. Tucci, E.S. Sobel, F. Silvestris, P. Tartaglia, et al., Induction of apoptosis by the hydrocarbon oil pristane: implications for pristane-induced lupus, J. Immunol. 175 (2005) 4777–4782.
[17] F. Geissmann, C. Auffray, R. Palframan, C. Wirrig, A. Ciocca, L. Campisi, et al., Blood monocytes: distinct subsets, how they relate to dendritic cells, and their possible roles in the regulation of T-cell responses, Immunol. Cell Biol. 86 (2008) 398–408.
[18] D. Kurotaki, N. Osato, A. Nishiyama, M. Yamamoto, T. Ban, H. Sato, et al., Essential role of the IRF8-KLF4 transcription factor cascade in murine monocyte differentiation, Blood 121 (2013) 1839–1849.
[19] O. Kulkarni, R.D. Pawar, W. Purschke, D. Eulberg, N. Selve, K. Buchner, et al., Spiegelmer inhibition of CCL2/MCP-1 ameliorates lupus nephritis in MRL-(Fas)lpr mice, J. Am. Soc. Nephrol. 18 (2007) 2350–2358.
[20] D.C. Nacionales, K.M. Kelly-Scumpia, P.Y. Lee, J.S. Weinstein, R. Lyons, E. Sobel, et al., Deficiency of the type I interferon receptor protects mice from experimental lupus, Arthritis Rheum. 56 (2007) 3770–3783.
[21] P. Blanco, A.K. Palucka, M. Gill, V. Pascual, J. Banchereau, Induction of dendritic cell differentiation by IFN-alpha in systemic lupus erythematosus, Science 294 (2001) 1540–1543.
[22] E. Zigmond, C. Varol, J. Farache, E. Elmaliah, A.T. Satpathy, G. Friedlander, et al., Ly6C hi monocytes in the inflamed colon give rise to proinflammatory effector cells and migratory antigen-presenting cells, Immunity 37 (2012) 1076–1090.
[23] N.V. Serbina, T.P. Salazar-Mather, C.A. Biron, W.A. Kuziel, E.G. Pamer, TNF/iNOS-producing dendritic cells mediate innate immune defense against bacterial infection, Immunity 19 (2003) 59–70.
[24] N.V. Serbina, E.G. Pamer, Monocyte emigration from bone marrow during bacterial infection requires signals mediated by chemokine receptor CCR2, Nat. Immunol. 7 (2006) 311–317.
[25] I.R. Dunay, R.A. Damatta, B. Fux, R. Presti, S. Greco, M. Colonna, et al., Gr1(+) inflammatory monocytes are required for mucosal resistance to the pathogen Toxoplasma gondii, Immunity 29 (2008) 306–317.
[26] M.A. Lowes, F. Chamian, M.V. Abello, J. Fuentes-Duculan, S.L. Lin, R. Nussbaum, et al., Increase in TNF-alpha and inducible nitric oxide synthase-expressing dendritic cells in psoriasis and reduction with efalizumab (anti-CD11a), Proc. Natl. Acad. Sci. U.S.A. 102 (2005) 19057–19062.
[27] L. Ronnblom, G.V. Alm, An etiopathogenic role for the type I IFN system in SLE, Trends Immunol. 22 (2001) 427–431.
[28] L. Ronnblom, G.V. Alm, M.L. Eloranta, Type I interferon and lupus, Curr. Opin. Rheumatol. 21 (2009) 471–477.
[29] J. Banchereau, V. Pascual, Type I interferon in systemic lupus erythematosus and other autoimmune diseases, Immunity 25 (2006) 383–392.
[30] J.J. Hooks, H.M. Moutsopoulos, S.A. Geis, N.I. Stahl, J.L. Decker, A.L. Notkins, Immune interferon in the circulation of patients with autoimmune disease, N. Engl. J. Med. 301 (1979) 5–8.
[31] E.C. Baechler, F.M. Batliwalla, G. Karypis, P.M. Gaffney, W.A. Ortmann, K.J. Espe, et al., Interferon-inducible gene expression signature in peripheral blood cells of patients with severe lupus, Proc. Natl. Acad. Sci. U.S.A. 100 (2003) 2610–2615.
[32] L. Bennett, A.K. Palucka, E. Arce, V. Cantrell, J. Borvak, J. Banchereau, et al., Interferon and granulopoiesis signatures in systemic lupus erythematosus blood, J. Exp. Med. 197 (2003) 711–723.
[33] R. Baccala, R. Gonzalez-Quintial, A.L. Blasius, I. Rimann, K. Ozato, D.H. Kono, et al., Essential requirement for IRF8 and SLC15A4 implicates plasmacytoid dendritic cells in the pathogenesis of lupus, Proc. Natl. Acad. Sci. U.S.A. 110 (2013) 2940–2945.
[34] T. Lovgren, M.L. Eloranta, U. Bave, G.V. Alm, L. Ronnblom, Induction of interferon-alpha production in plasmacytoid dendritic cells by immune complexes containing nucleic acid released by necrotic or late apoptotic cells and lupus IgG, Arthritis Rheum. 50 (2004) 1861–1872.
[35] H. Zhuang, C. Szeto, S. Han, L. Yang, W.H. Reeves, Animal models of interferon signature positive lupus, Front. Immunol. 6 (2015) 291.
[36] H. Negishi, T. Taniguchi, H. Yanai, The interferon (IFN) class of cytokines and the IFN regulatory factor (IRF) transcription factor family, Cold. Spring. Harb. Perspect. Biol. 10 (11) (2018).
[37] D. Kurotaki, T. Tamura, Transcriptional and epigenetic regulation of innate immune cell development by the transcription factor, interferon regulatory factor-8, J. Interferon Cytokine Res. 36 (2016) 433–441.
[38] H. Tsujimura, T. Tamura, K. Ozato, Cutting edge: IFN consensus sequence binding protein/IFN regulatory factor 8 drives the development of type I IFN-producing plasmacytoid dendritic cells, J. Immunol. 170 (2003) 1131–1135.
[39] J. Aliberti, O. Schulz, D.J. Pennington, H. Tsujimura, C. Reis e Sousa, K. Ozato, et al., Essential role for ICSBP in the in vivo development of murine CD8alpha + dendritic cells, Blood 101 (2003) 305–310.
[40] M. Scheller, J. Foerster, C.M. Heyworth, J.F. Waring, J. Lohler, G.L. Gilmore, et al., Altered development and cytokine responses of myeloid progenitors in the absence of transcription factor, interferon consensus sequence binding protein, Blood 94 (1999) 3764–3771.
[41] C.H. Lee, M. Melchers, H. Wang, T.A. Torrey, R. Slota, C.F. Qi, et al., Regulation of the germinal center gene program by interferon (IFN) regulatory factor 8/IFN consensus sequence-binding protein, J. Exp. Med. 203 (2006) 63–72.
[42] P.Y. Lee, Y. Li, Y. Kumagai, Y. Xu, J.S. Weinstein, E.S. Kellner, et al., Type I interferon modulates monocyte recruitment and maturation in chronic inflammation, Am. J. Pathol. 175 (2009) 2023–2033.
[43] P.Y. Lee, N. Nelson-Maney, Y. Huang, A. Levescot, Q. Wang, K. Wei, et al., High-dimensional analysis reveals a pathogenic role of inflammatory monocytes in experimental diffuse alveolar hemorrhage, J.C.I. Insight. 4 (15) (2019).
[44] T. Luft, K.C. Pang, E. Thomas, P. Hertzog, D.N. Hart, J. Trapani, et al., Type I IFNs enhance the terminal differentiation of dendritic cells, J. Immunol. 161 (1998) 1947–1953.